Computation of Flows Around a High Speed Catamaran

Seung-Hyun Kwag*
School of Mechanical Engineering, Halla University

A numerical study is carried out to clarify the characteristics of flow fields and breaking phenomena around a high speed catamaran hull advancing on calm water. Computations are carried out for Froude numbers between 0.2 and 1.0 and for ratios of the distance between hulls to the catamaran length varying between 0.2 and 0.5 for a mathematically defined Wigley hull. A Navier-Stokes solver which includes the nonlinearities of free surface conditions is employed. Computations are performed in a rectangular grid system based on the Marker & Cell method. For validation, present computation results are compared with existing experimental results. As an application, the results of the displacement catamaran are used for the breaking analysis.

Key Words: Catamaran, Free Surface, Navier-Stokes Solver, Third Derivative Upwind, Wave Sub-Breaking, Wave Body Viscous Interaction

1. Introduction

Free surface handling and wave-body interaction are impotant for designing high speed vessels, especially passenger ferries. Recently various hull forms such as hydrofoil crafts, planing boats, catamaran and surface effect ships have been developed. Catamaran is one of the most practical hull forms due to the large deck area with small waterplane area, good transverse stability quality, and unusual resistance property.

Although a number of experimental and theoretical investigations (Insel(1991), Eggers(1995), Turner(1968), Everest(1967/8), Fry(1972), Harries (1997), Helmerson(1991)) on the catamaran resistance were conducted in the past, the understanding of interference effects between demihulls is lacking. Furthermore, there are only a few publications available for displacement catamarans at speeds greater than Fn=0.5, which is representative of modern high speed displacement catamarans. Among recent experimental investigations, Insel(1991) gained good results for wave resistance of catamaran with varying separation lengths and Froude numbers. The wave resistance characteristics of a catamaran, are affected by the length-displacement ratio, demihull spacing, initial trim, and hull form. For high speed ships, the main resistance is the wave resistance.

Generally, two types of interference resistances are known. First type is viscous interference caused by asymmetric flow around demihulls and its effect on boundary layer formation and the vortices development. Second type is the wave interference resistance originating from the interaction between the wave systems of demihulls. For a high speed catamaran, the velocity difference between the inner and outer sides of the demihull makes the analysis of wave resistance difficult.

In the present paper, the wave interference is numerically investigated and the optimum hull spacing for minimum wave interference is found by varying s/L over a wide range of Froude numbers. The results are compared with the existing experimental data (Insel, 1991). Using the numerical results, the breaking phenomenon is studied for a displacement catamaran because the breaking is closely related to the free surface

* **E-mail** : shkwag@hit.halla.ac.kr
TEL : +82-33-760-1233 **FAX** : +82-33-760-1361
School of Mechanical Engineering, Halla University, 66 Heungup, Wonju, Kangwondo 220-712 Korea.(Manuscript **Received** April 14, 2000; **Revised** January 3, 2001)

turbulent flows.

2. Numerical Scheme

2.1 Basic equations

Numerical simulations of 3-D free-surface flows are carried out by using the MAC method. The velocity components u, v and w at (n+1) time step are determined by

$$u^{n+1}=(F^n-\phi_x^n)\Delta t$$
$$v^{n+1}=(G^n-\phi_y^n)\Delta t$$
$$w^{n+1}=(H^n-\phi_z^n)\Delta t \tag{1}$$

where

$$F^n=\frac{u^n}{\Delta t}+\left(\frac{1}{Re}+v_t\right)\nabla^2 u - \left(u^n\frac{\partial u}{\partial x}+v^n\frac{\partial u}{\partial y}+w^n\frac{\partial u}{\partial z}\right) - \frac{\partial}{\partial x}\left(v_t\left(2\frac{\partial u}{\partial x}\right)\right) - \frac{\partial}{\partial y}\left\{v_t\left(\frac{\partial u}{\partial y}+\frac{\partial v}{\partial x}\right)\right\} - \frac{\partial}{\partial z}\left(v_t\left(\frac{\partial u}{\partial z}+\frac{\partial w}{\partial x}\right)\right)\Big\}$$

$$G^n=\frac{v^n}{\Delta t}+\left(\frac{1}{Re}+v_t\right)\nabla^2 v - \left(u^n\frac{\partial v}{\partial x}+v^n\frac{\partial v}{\partial y}+w^n\frac{\partial v}{\partial z}\right) - \frac{\partial}{\partial x}\left(v_t\left(\frac{\partial u}{\partial y}+\frac{\partial v}{\partial x}\right)\right)\Big\} - \frac{\partial}{\partial y}\left(v_t\left(2\frac{\partial v}{\partial y}\right)\right)\Big\} - \frac{\partial}{\partial z}\left(v_t\left(\frac{\partial v}{\partial z}+\frac{\partial w}{\partial y}\right)\right)\Big\} \tag{2}$$

$$H_n=\frac{w^n}{\Delta t}+\left(\frac{1}{Re}+v_t\right)\Delta w - \left(u^n\frac{\partial w}{\partial x}+v^n\frac{\partial w}{\partial y}+w^n\frac{\partial w}{\partial z}\right) - \frac{\partial}{\partial x}\left(v_t\left(\frac{\partial u}{\partial z}+\frac{\partial w}{\partial x}\right)\right)\Big\} - \frac{\partial}{\partial y}\left\{v_t\left(\frac{\partial v}{\partial z}+\frac{\partial w}{\partial y}\right)\right\} - \frac{\partial}{\partial z}\left\{v_t\left(2\frac{\partial w}{\partial z}\right)\right\}$$

and

$$\Phi^n=p+\frac{z}{Fn^2} \tag{3}$$

$$\Delta^2=\frac{\partial}{\partial x^2}+\frac{\partial}{\partial y^2}+\frac{\partial}{\partial z^2} \tag{4}$$

Differentiating Eq. (1) with respect to x, y and z,

$$\Delta^2\Phi=F_x+G_y+H_z - \left(u_x^{n+1}+v_y^{n+1}+w_z^{n+1}\right)/\Delta t \tag{5}$$

The last term in Eq. (5) is expected to be zero to satisfy the continuity condition. Equation (5) can be solved by a relaxation method.

It is desirable to introduce coordinate transformations which simplify the computational domain in the transformed domain

$$\xi=\xi(x, y, z),\ \eta(x, y, z),\ \zeta=\zeta(x, y, z) \tag{7}$$

Through transformations, Eq. (1) can be written,

$$q_t+Uq_\xi+Vq_\eta+Wq_\zeta = \left(\frac{1}{Re}+v_t\right)\nabla^2 q-K-REYSF(\xi, \eta, \zeta) \tag{8}$$

where U, V and W are the contravariant velocities and K is the pressure gradient. The pressure is calculated by the following relaxation formula,

$$\Phi^{m+1}=\Phi^m+\omega\cdot(\Phi^{m+1}-\Phi^m) \tag{9}$$

where $(m+1)$ denotes the next time step and ω is the relaxation factor.

2.2 Computational procedure and boundary conditions

The Navier-Stokes(N-S) and Poisson equations are solved after the transformation. The calculation proceeds through a sequence of loops each advancing the entire flow configuration by a sufficiently small finite time increment. The output of each loop is taken as the initial condition for the next step, and computation is performed until steady state is reached. An explicit Euler scheme is used for the time marching procedure. Pressure is obtained throughout the fluid domain by solving the Poisson equation. Iterations are automatically stopped when the pressure difference between two consecutive approximations is smaller than a previously chosen quantity ε. The velocity field is updated by using a time-forward difference form of the momentum equations.

The third order upstream difference is used for convection terms with the fourth-order truncation error, for example;

$$
\begin{aligned}
&U\cdot(\delta f/\delta x)_{i,j,k}\\
&=U_{i,j,k}\cdot(f_{i-2,j,k}-8f_{i-1,j,k}+8f_{i+1,j,k}\\
&-f_{i+2,j,k})/12\\
&+|U_{i,j,k}|\cdot(f_{i-2,j,k}-4f_{i-1,j,k}+6f_{i,j,k}\\
&-4f_{i+i,j,k}+f_{i+2,j,k})/4
\end{aligned}
\tag{10}
$$

As boundary conditions, the following are used.

Upstream

$$u=1,\ v=0,\ w=0 \text{ and } p=0$$
$$\Delta u=\Delta v=\Delta w=0$$

Downstream

$$u_\ell=v_\ell=w_\ell=0$$
$$\Delta u_\ell=\Delta v_\ell=\Delta w_\ell=\Delta p_\ell=0$$

Symmetrical

$$u_\eta=v_\eta=w_\eta=0$$
$$\Delta u_\eta=\Delta v_\eta=\Delta w_\eta=\Delta p_\eta=0$$

Body surface

$$u=v=w=0,\ p_\zeta=0$$
$$\Delta u=\Delta v=\Delta w=0,\ \Delta p_\zeta=0$$

2.3 Free surface boundary condition

The fluid particle motion on a free surface is given by

$$\frac{\partial h}{\partial t}+u\frac{\partial h}{\partial x}-w=0\,|_{z=\zeta} \tag{11}$$

The free surface boundary condition requires zero tangential stress and a normal stress that balances any externally applied normal stress. The particle displacement is given by

$$\Delta x=u\cdot\Delta t,\ \Delta h=w\cdot\Delta t \tag{12}$$

where Δt is the time increment. On the other hand, the use of an Euler-type expression of the kinematic free surface boundary condition makes it possible to employ a higher finite difference scheme. This condition can be written as follows:

$$\frac{\partial h_i^{n+1}}{\partial t}+\left(u_i+\frac{\partial u_i}{\partial z}\Delta h_i\right)\cdot\frac{\partial h_i^{n+1}}{\partial x}-w_i=0 \tag{13}$$

where $h=h(x,\ h)$ represents the elevation. Expanding in Taylor series, the derivative term can be discretized by using Eq. (14).

$$\partial h_i^{n+1}=\frac{1}{2\Delta t}\cdot(h^{n-1}-4h^n+3h^{n+1}) \tag{14}$$

For the $\partial h^{n+1}/\partial x$ derivative, the third order upwind difference (TOUD) is adopted.

$$c\frac{\partial h}{\partial x}=c\frac{1}{6\Delta x}(-2h_{i-3}+9h_{i-2}-18h_{i-1}+11h_i) \tag{15}$$

where c is the convective velocity which can be decomposed into two parts. One is the central differencing term whose mathematical expression can be obtained by suitable Taylor expansions as follows:

$$\frac{c}{24\Delta x}(h_{i-3}-27h_{i-2}+27h_{i-1}-h_i) \tag{16}$$

The other is the diffusion term, which is the fourth derivative of velocity.

$$\frac{3c}{8\Delta x}(-h_{i-3}+7h_{i-2}-11h_{i-1}+5h_i) \tag{17}$$

The latter is expected to eliminate phere shift due to differentiation. Similarly, the third derivative, Eq. (18), also reduces phase shift and damping. It is also obtained by Taylor expansions as follows:

$$\frac{ac}{(\Delta x)^3}(-h_{i-3}+3h_{i-2}-3h_{i-1}+h_i) \tag{18}$$

where $a=-\dfrac{(\Delta x)^2}{6}$ is a constant.

Equation (18) is added to the right handed side of Eq. (15), and the new formulation for the $\partial h/\partial x$ becomes,

$$
\begin{aligned}
c\frac{\partial h}{\partial x}&=c\frac{1}{6\Delta x}(-h_{i3}+6h_{i-2}-15h_{i-1}+10h_i)\\
&\frac{ac}{(\Delta x)^3}(-h_{i-3}+3h_{i-2}-3h_{i-1}+h_i)
\end{aligned}
\tag{19}
$$

Equation (19) is the same expression used by Dawson (1977) in his steady analysis using the Rankine source method where he derived $\partial h/\partial x$ without the third derivative terms. Introducing Eq. (14) and Eq. (19) into Eq. (13), the vertical coordinate increment at each time step is

$$
\Delta h_i^n=\frac{3\Delta x(h_i^n-h_i^{n-1}+\Delta t\cdot[6w_i\Delta x+u_i(\Delta h_{i-3}^n-6\Delta h_{i-2}^n+15\Delta h_{i-1}^n-Q_i^n)]}{9\Delta x+\Delta t\cdot[10u_i+Q_i^n\dfrac{\partial u}{\partial z}-6\Delta x\dfrac{\partial w}{\partial z}]}
\tag{20}
$$

The expression is of the second order accuracy for $h(0(h^2))$ for any $u>0$. $Q^n{}_i$ in Eq. (20) is

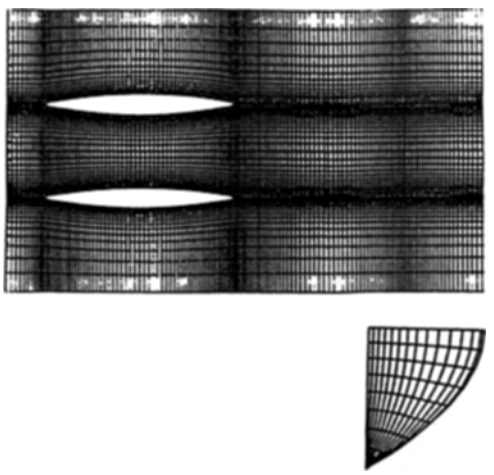

Fig. 1(a) Grid generation for Wigley ship model

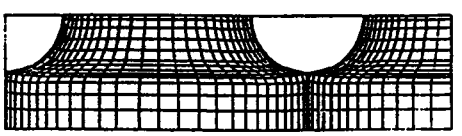

Fig. 1(b) Grid generation for catamaran

$$Q_i^n = -h_{i-3}^n + 6h_{i-2}^n - 15h_{i-1}^n + 10h_i^n \quad (21)$$

where h at the $(n+1)^{th}$ step is calculated as

$$h^{n+1} = h^n + \Delta h^n \quad (22)$$

3. Results and Discussion

3.1 Results of Wigley-shaped catamaran

The catamaran with Wigley demihulls was tested at Froude numbers 0.289, 0.316, 0.5, 0.6 1. 0 and s/L of 0.2, 0.3 0.5 in which s is the distance between hulls and L is the length of catamaran. Figure 1(a) shows the grid view for Wigley-shaped catamaran where the grid size is 104x48x23. Figure 1(b) is for the displacement catamaran whose grid sizes are 80x16x16 for the mono hull and 80x30x16 for the twin hull. The time increment Δt is 0.0005. However, more severe time increment condition than Courant condtion should be used because both convection and diffusion terms are treated explicitly. Also the Baldwin - Lomax turbulence model is used.

For the computation domain, half of the ship length is occupied in the lateral direction and the distance greater than the length of catamaran in the downstream direction. The grid is made of H-H topology to treat the free surface movement more conveniently. The wave height contours are shown in Fig. 2 and Fig. 3 for different Froude numbers and s/L's. As the s/L decreases, the divergent wave between demihulls is eliminated and the transverse wave becomes dominant due to the divergent wave interference. For s/L=0.5, the wave interference almost disappears and the wave pattern becomes similar to that of a monohull. The effect of wave interference between demihulls becomes dominant as the s/L dicreases. For s/L =0.2, as the wave interference become larger, the effect is propagated into the outer flow region

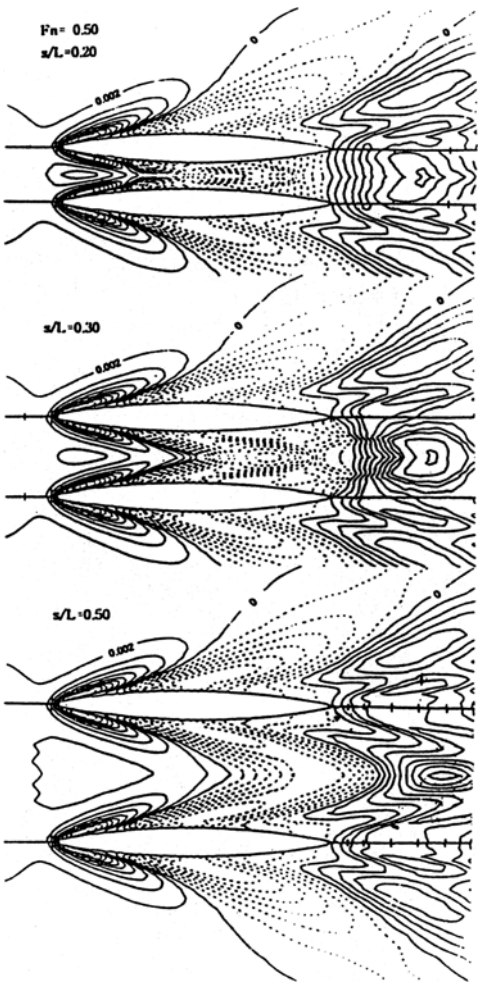

Fig. 2 Wave height contour at $Fr=0.50$ for s/L=0. 20, 0.30, 0.50

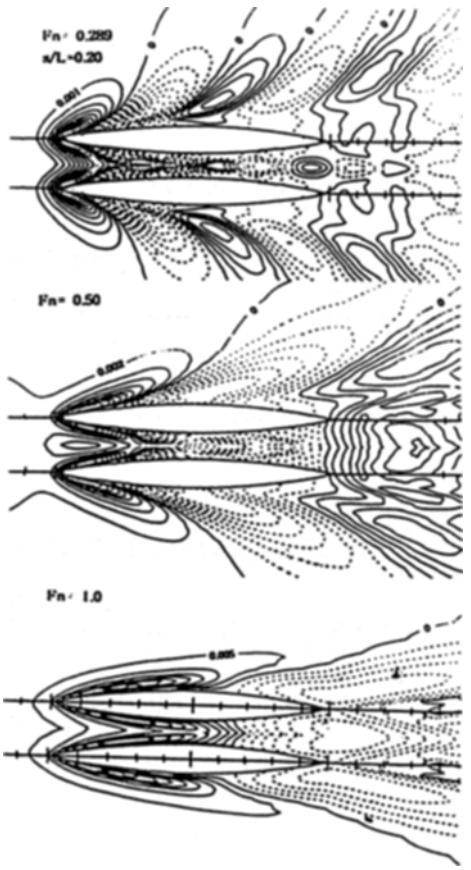

Fig. 3 Wave height contour at s/L=0.20 for Fr=0.50, 0.50, 1.0

from the demihulls. In Fig. 4, the computed resistance is compared with the results from (Insel & Molland, (1991) and potential theory of Shin (1994). The results agree qualitatively with data. The wave resistance interference factors τ, for different s/L's, are given in Fig. 5, which are defined as C_W(catamaran)/C_W(monohull). Although the computed data points are insufficient, the wave interference factors agree well with experimental data for s/L=0.3 and Fr=0.6. At s/L=0.5, the wave interference factors agree even at the highest Froude number. Therefore the wave interference can be effectively applied to design high speed catamarans by using Eqs. (23)~(26).

3.2 Result of displacement catamaran

Another example is the displacement

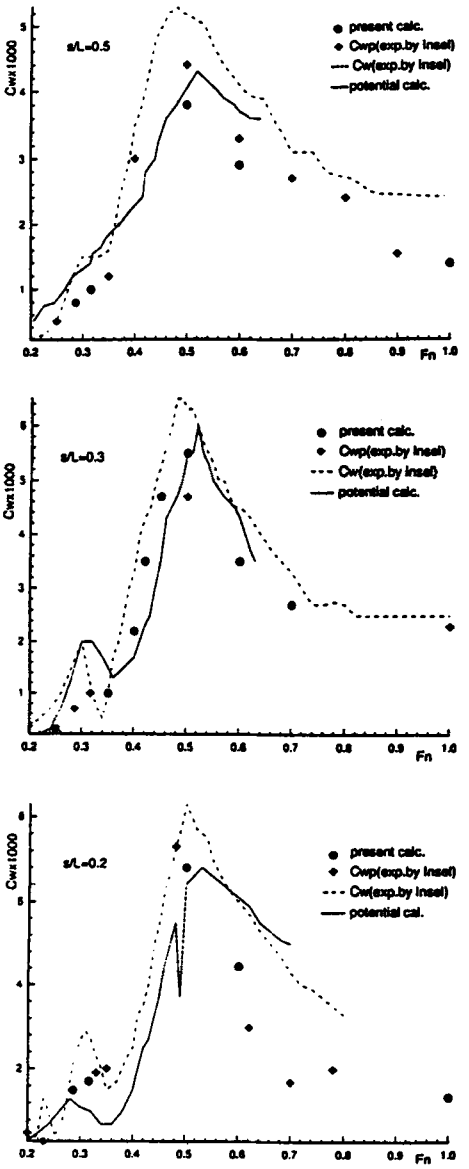

Fig. 4 Wave resistance coefficient Cw for s/L=0.50, 0.30, 0.20

catamaran moving at Froude numbers of 0.45, and 0.95. Figure 6 shows a comparison of monohull results(a and b) and twin-hull in results (c). The effects of Froude number are clear. Figure 7 shows the wave heights for mono hulls and a catamaran. Due to insufficient computation domain, the reflection wave is seen near the rear-lateral side. Velocity vectors inside and

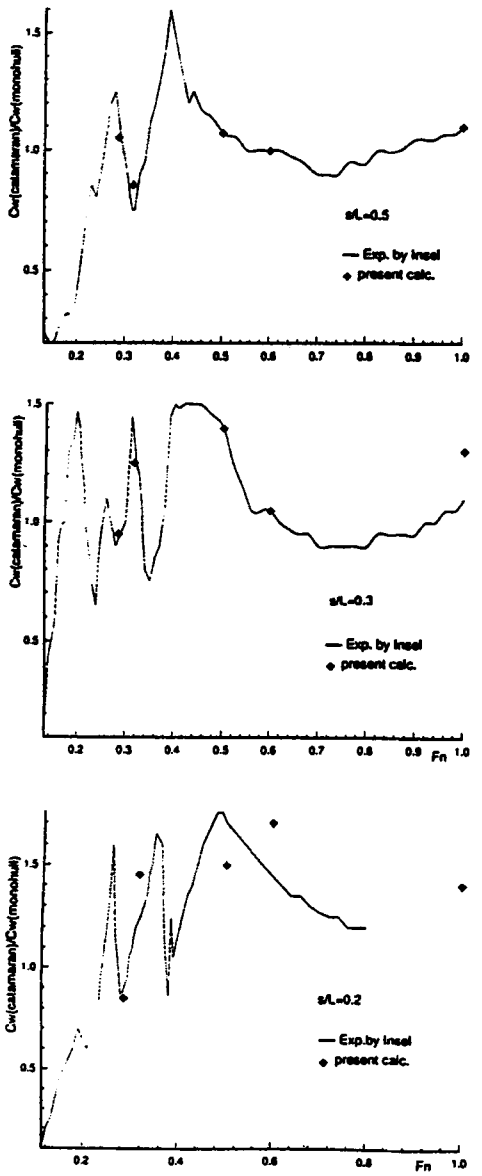

Fig. 5 Wave resistance interference factor τ

outside the hulls can be seen in Fig. 8.

3.3 Detection of sub-breaking waves

As an application, sub-breaking waves are numerically detected in free surface flows around a submerged hydrofoil. The sub-breaking waves are waves caused by instabilities in the free surface flow. An instability analysis (Mori, 1988) provides a critical condition for their appearance.

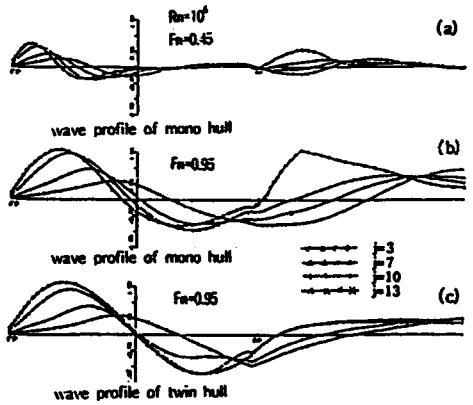

Fig. 6 Wave height comparison between mono and twin hulls

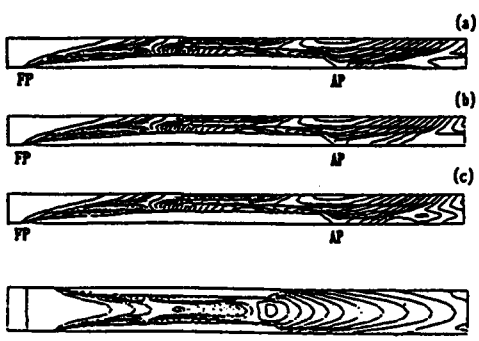

Fig. 7 Wave height comparison for a mono hull (a) $t=2.0$ (b) $t=2.5$ (c) $t=3.0$ and the wave contour for a catamaran at $t=3.0$

$$\frac{U}{M}\frac{\delta M}{h\delta s}-\frac{\delta U}{h\delta s}-\frac{1}{n_z}\frac{\delta n_z}{h\delta s}>0 \tag{23}$$

where

$$M=(\kappa U^2-n_z\cdot g)\cdot n_z \tag{24}$$

The streamline coordinate along and normal to the free surface are denoted by s and n, respectively. The metric coefficient along s is h, and ; n_z is the direction cosine of n to z. Uo is the velocity component in the s-direction. κ is the curvature of the free surface, and g is the gravity acceleration. In a narrow region near the wave crest, we assume $n_z=1$ and $\delta/h\delta s=\delta/\delta x$, then Eq. (13) can be reduced approximately to

$$\frac{U}{M}\frac{\partial M}{\partial x}\frac{}{U}>0 \tag{25}$$

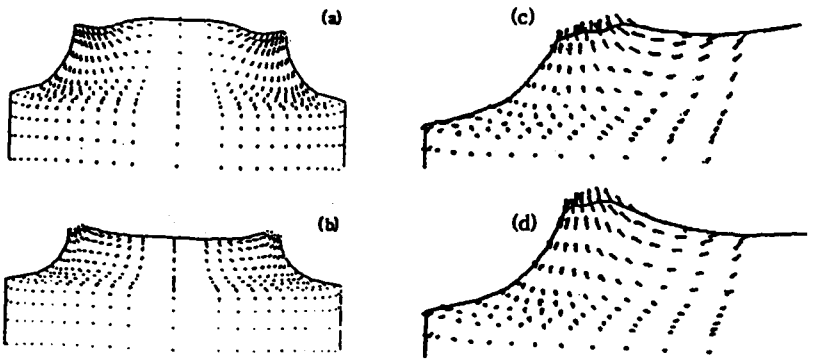

Fig. 8 Velocities inside and outside the hulls (a) x/L=0.55 (b) 0.90 (c) 0.88 (d) 0.93

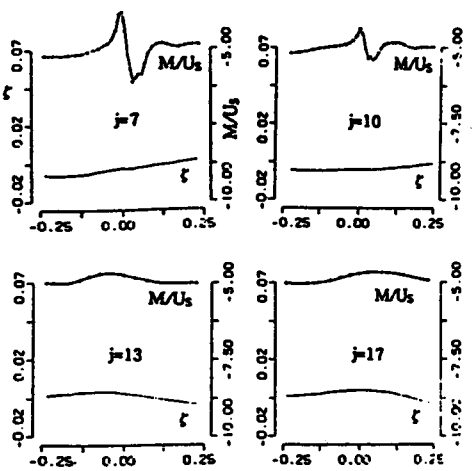

Fig. 9 Breaking analysis for a mono hull M/U_s and free-surface amplitude

where

$$M=\kappa U_0^2-g \tag{26}$$

M is negative; therefore, the negative gradient of M/U along x suggests the possibility of instability in the free surface. Steep negative gradient can be seen as the speed increases and the wave breaking can be serious at the Froude number of 0.95. Figures 9 and 10 show the breaking analysis results for mono and twin hulls at $Fr=$ 0.95. The breaking is more serious for a catamaran than mono hulls, especially near the hull surface. Figure 11 shows the photos of stern waves at three speeds, which were taken in the towing basin of Hyundai Maritime Research Institute.

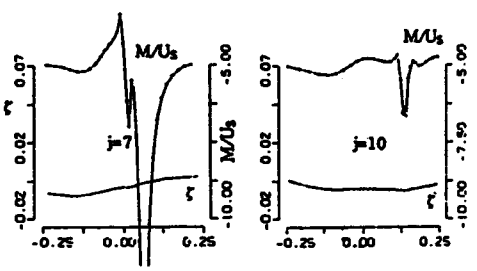

Fig. 10 Breaking analysis for a twin hull M/U_s and free-surface amplitude

4. Conclusion

(1) The flow characteristics for a high speed catamaran has been numerically investigated and compared against experimental data. The effect of wave interference has been reviewed and the optimum hull spacing for minimum wave interference at various Froude numbers has been found.

(2) Numerical analysis of breaking waves have been carried out. Instabilities can be found near demihulls instead of monohulls. A steep negative gradient can be seen as the speed increases, and the wave breaking is more serious at larger Froude numbers.

(3) The calculated stern waves are similar to those from experiments in a towing basin. The stern waves generated behind have an influence on the total wave resistance, which is a function of the high speed catamaran design.

Fig. 11 Photos for stern waves of catamaran 4.0m/sec, 4.5m/sec, 5.0m/sec from l.h.s.

References

Dawson, C.W., 1977, "A Practical Computer Method for Solving Ship Wave Problems," *Proc. 2nd Int. Conf. on Num. Ship Hydro.*, Univ. of California, Berkeley, pp. 30~38.

Eggers, K., 1995, "Resistance Conditions of Two-Body Ships," *Jahrbuch der Schiffbautech Gesellshaft*, Vol. 49.

Everest, J.T., 1967/8, "Some Research on the Hydrodynamics of Catamarans and Multi- Hulled Vessels in Calm Water," *Trans. NECIES*, Vol. 84.

Fry, E.D. and Graul, T., 1972, "Design and Application of Modern High-Speed Catamarans," *Marine Technology*, Vol. 9, No. 3.

Harries, S. and Schulze, D., 1997, "Numerical Investigation of a Systematic Model Series for the Design of Fast Monohulls," FAST '97

Helmerson, H. and Werenskiold, P., 1991, "Safety of Fast Sea Transport," FAST '91, pp. 1297~1313.

Insel, H. and Molland, A.F., 1991, "An Investigation into the Resistance of High Speed Displacement Catamarans," *Trans, RINA*

Lewthwaite, J.C., Stintion, D. and Wardale, A. T., 1994, "Likely Developments in Large High Speed Ferries by the Year 2000," FFI

Mori, K., Shin, M., 1988, "Sub-breaking Wave: Its Characteristics, Appearing Condition and Numerical Simulation," *Proc. 17th Symp on Naval Hydro, ONR Research.*

Shin, M.S., Lee, S.J., Wee, C.W., 1994, "A Nonlinear Calculation of Wave Resistance for Catamarans," *Proc. of Soc. of Naval Arch. of Korea*, pp. 364~370.

Turner, H. and Taplin, A. , 1968, "The Resi stance of Large Powered Catamarans," *Trans. SNAME*, Vol. 76.